journal

J. Am. Ceram. Soc., **74** [12] 3061–65 (1991)

Phase Stability and Physical Properties of Cubic and Tetragonal ZrO$_2$ in the System ZrO$_2$–Y$_2$O$_3$–Ta$_2$O$_5$

Dae-Joon Kim*

Ceramics Division, Korea Institute of Science and Technology, Seoul, Korea

Tseng-Ying Tien*

Department of Materials Science and Engineering, The University of Michigan,
Ann Arbor, Michigan 48104

The cubic (c-ZrO$_2$) and tetragonal zirconia (t-ZrO$_2$) phase stability regions in the system ZrO$_2$–Y$_2$O$_3$–Ta$_2$O$_5$ were delineated. The c-ZrO$_2$ solid solutions are formed with the fluorite structure. The t-ZrO$_2$ solid solutions having a c/a axial ratio (tetragonality) smaller than 1.0203 display high fracture toughness (5 to 14 MPa·m$^{1/2}$), and their instability/transformability to monoclinic zirconia (m-ZrO$_2$) increases with increasing tetragonality. On the other hand, the t-ZrO$_2$ solid solutions stabilized at room temperature with tetragonality greater than 1.0203 have low toughness values (2 to 5 MPa·m$^{1/2}$), and their transformability is not related to the tetragonality. [Key words: zirconia, solid solution, lattice, phases, physical properties.]

I. Introduction

THE alloying of Y$_2$O$_3$ into ZrO$_2$ stabilizes the high-temperature phases, cubic ZrO$_2$ (c-ZrO$_2$) and tetragonal ZrO$_2$ (t-ZrO$_2$), by suppressing the deleterious phase transformation to monoclinic ZrO$_2$ (m-ZrO$_2$) which is the room-temperature-stable form of the pure ZrO$_2$. The substitution of Y^{3+} for Zr^{4+} in the formation of the solid solutions results in a creation of oxygen-ion vacancies to balance the change in valence. The fluorite structure c-ZrO$_2$, alloyed with more than 8 mol% Y$_2$O$_3$, is a stable phase at ambient temperature and has been used as ionic conductors. The distorted fluorite structure t-ZrO$_2$, alloyed with about 2 to 3 mol% Y$_2$O$_3$, is a metastable phase at room temperature and has been considered as a structural ceramic because of its excellent mechanical properties, such as fracture toughness, strength, and hardness.

The stability regions and the ionic conductivities of c-ZrO$_2$ in the system ZrO$_2$–Y$_2$O$_3$–Ta$_2$O$_5$[1] and the related ternary system ZrO$_2$–MgO–Ta$_2$O$_5$[2] are of interest mainly because the alloying of Ta$_2$O$_5$ into c-ZrO$_2$ in the binary systems is expected to suppress the oxygen-ion vacancy formation as a result of the substitution of Ta^{5+} for Zr^{4+}. On the other hand, recently a small amount of Ta$_2$O$_5$ or Nb$_2$O$_5$ alloying into t-ZrO$_2$ in the system ZrO$_2$–Y$_2$O$_3$ was found to remarkably increase its fracture toughness, which is related to the increase in the tetragonality of t-ZrO$_2$ symmetry.[3] While technologically important, the studies of phase relationships in ternary systems with pentavalent oxides are either incomplete or lack details about the stability of t-ZrO$_2$ solid solutions.[1,2,4]

The purpose of this study is to investigate the phase stability regions of c-ZrO$_2$ and t-ZrO$_2$ and the mechanical and crystallochemical properties of t-ZrO$_2$ alloys in the system ZrO$_2$–Y$_2$O$_3$–Ta$_2$O$_5$.

II. Experimental Procedure

The starting powders were prepared by the coprecipitation from aqueous solutions of ZrOCl$_2$·8H$_2$O, Y(NO$_3$)$_3$·6H$_2$O, and TaCl$_5$ using ammonia. The coprecipitation was accomplished at pH 7.6 by pouring the aqueous mixture into vigorously stirred ammonia. The precipitates were dried for 20 h at 120°C after washing with distilled water and decomposed to the oxides by calcination for 3 h at 920°C. The oxide agglomerates were attrition-milled using ZrO$_2$ balls. Pellets of each composition were fired on platinum foil at 1500°C for up to 165 h. The fired pellets were examined by X-ray diffraction (XRD) for phase equilibria. The fracture toughness was determined by the indentation technique using the equation proposed by Anstis *et al.*[5] The Young's modulus was calculated from the bulk density, and the longitudinal and transverse wave velocity measured with an ultrasonic transducer.[6] The bulk density of specimens was determined by the Archimedes method. A dilatometer was used to measure the phase transformation temperatures of m-ZrO$_2$ → t-ZrO$_2$ (A$_s$) and t-ZrO$_2$ → m-ZrO$_2$ (M$_s$) which correspond to the starting points of the discontinuous volume shrinkage and expansion of the samples during heating and cooling, respectively. The dilatometry samples, which were prepared by pressing the powders isostatically at 170 MPa, were heated from room temperature to 1200°C and cooled at the same rate of 7.5°C/min. For lattice parameter determination, X-ray powder diffraction data from the pressed and sintered samples coated with a thin layer of Si powder (SRM640b) were obtained on a goniometer (2θ/θ, Scintag, Santa Clara, CA) equipped with a solid-state detector and a Cu X-ray tube, λ(CuKα$_1$) = 1.5405981 Å. A detail of the procedure and the X-ray powder diffraction data for t-ZrO$_2$ solid solutions in the system ZrO$_2$–YTaO$_4$ are described elsewhere.[7] The Raman spectra were obtained with the 514.5-nm line of a 0.35-W argon laser.

III. Results and Discussion

An isothermal section of the phase diagram for the system ZrO$_2$–Y$_2$O$_3$–Ta$_2$O$_5$ at 1500°C is determined and illustrated in Fig. 1. The dome-shape c-ZrO$_2$ phase region is consistent with the stability boundary reported by Choudhary and Subbarao,[1] and a similar ternary t-ZrO$_2$ phase field is also found in the system ZrO$_2$–MgO–Ta$_2$O$_5$.[2] In Fig. 2 the lattice parameters of c-ZrO$_2$ solid solutions in the system ZrO$_2$–Y$_2$O$_3$–Ta$_2$O$_5$, measured by Choudhary and Subbarao,[1] are compared with the calculated values from the empirical equation for the fluorite structure c-ZrO$_2$ solid solutions.[8] With the ionic radii in eightfold coordination, that is, $r_{Zr^{4+}}$ =
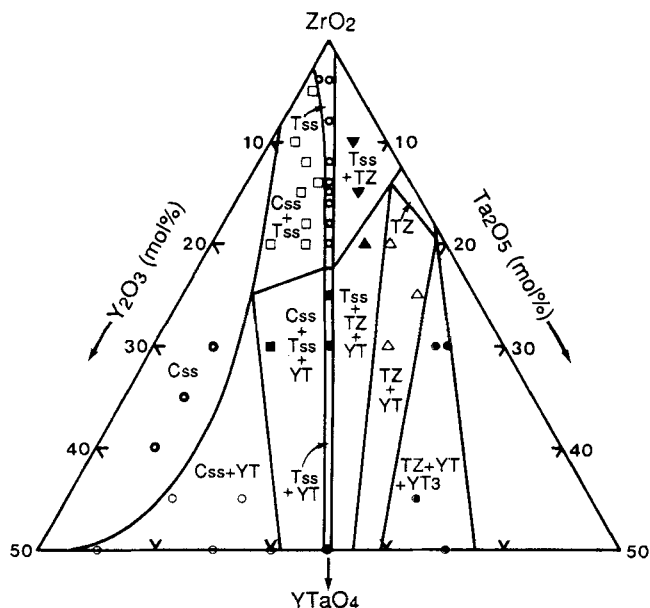
ZrO₂

Fig. 1. Part of the ternary phase diagram for the system ZrO₂–Y₂O₃–Ta₂O₅ at 1500°C. *T*ss is *t*-ZrO₂ solid solution, *C*ss is *c*-ZrO₂ solid solution, TZ is Ta₂Zr₆O₁₇, YT is YTaO₄, YT₃ is YTa₃O₉.

0.84 Å, $r_{Y^{3+}}$ = 1.019 Å, and $r_{Ta^{5+}}$ = 0.74 Å,[9] the equation for the lattice constants (in Å) can be written as

$$d = 5.120 + 0.00141m_Y + 0.00027m_{Ta} \qquad (1)$$

where m_Y and m_{Ta} are mol% of YO₁.₅ and TaO₂.₅, respectively. The remarkable agreement between the measured and the calculated lattice constants in Fig. 2 suggests that Y³⁺ and Ta⁵⁺ are randomly substituted for Zr⁴⁺ in 8-fold lattice sites of the fluorite structure.

The effect of Ta₂O₅ alloying on the phase stability of *c*-ZrO₂ is shown in Fig. 3(A), where Ta₂O₅ was increasingly added to 8 mol% Y₂O₃-stabilized *c*-ZrO₂. The Ta₂O₅ alloying in the *c*-ZrO₂ results in the decrease of the phase stability of *c*-ZrO₂, which is indicated by the diminishing XRD peak corresponding to *c*-ZrO₂ with increasing amount of Ta₂O₅. On the other hand, Fig. 3(B) shows the decrease in *t*-ZrO₂ stability by Ta₂O₅ alloying. The intensity of the XRD peak assigned to *t*-ZrO₂ becomes weak and those related to *m*-ZrO₂
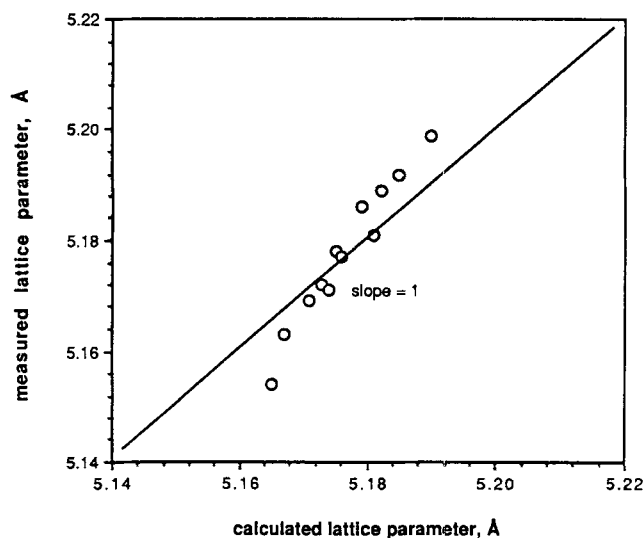

Fig. 2. Comparison of measured (Ref. 1) and calculated lattice parameters of cubic ZrO₂ solid solutions in the system ZrO₂–Y₂O₃–Ta₂O₅.
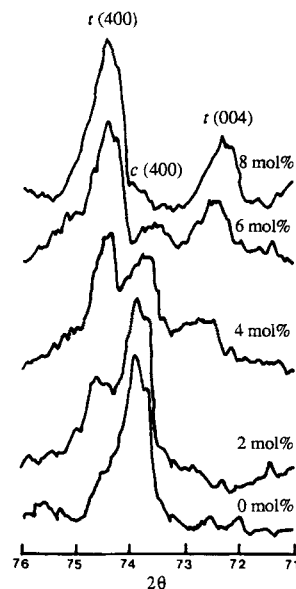

Fig. 3(a). Ta₂O₅ alloying effect on phase stability of 8 mol% Y₂O₃-stabilized cubic ZrO₂ after sintering for 5 h in 1500°C.

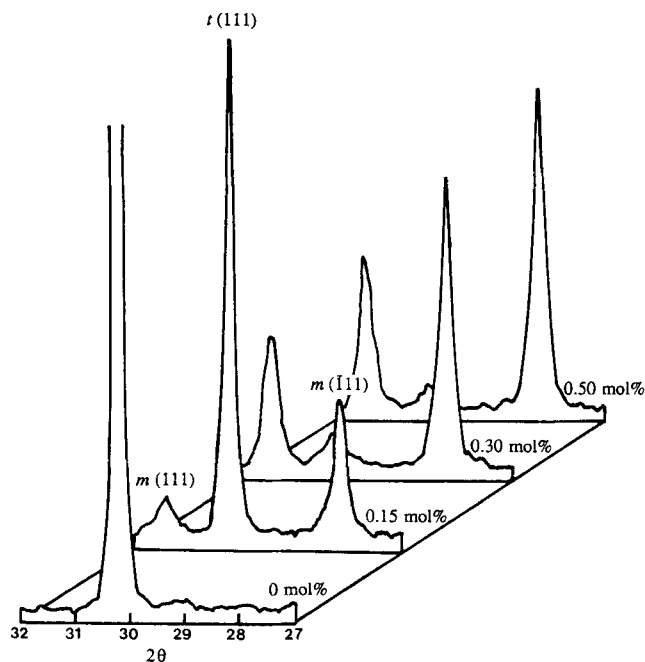**Fig. 3(b).** Ta₂O₅ alloying effect on phase stability of 2 mol% Y₂O₃-stabilized tetragonal ZrO₂ after sintering for 5 h at 1500°C.

become strong as the Ta₂O₅ alloying into 2 mol% Y₂O₃-stabilized *t*-ZrO₂ increases. The Ta₂O₅ alloying is reported to have little effect on the grain size of Y₂O₃-stabilized *t*-ZrO₂.[3] Thus, the Ta₂O₅ behaves as a destabilizer for the high-temperature phases of ZrO₂.

The quasi-binary system ZrO₂–YTaO₄ is unique because the crystallochemical characteristics of ZrO₂ are similar to those of YTaO₄, which has a monoclinic distorted scheelite structure at ambient temperature and transforms to a tetragonal scheelite form above 1400°C.[10] The *t*-ZrO₂ single-phase region in Fig. 1 extends to about 22 mol% YTaO₄, which corresponds to 0.78ZrO₂·0.11Y₂O₃·0.11Ta₂O₅. This *t*-ZrO₂ stability boundary is more extensive than that in the analogous system ZrO₂–MgTa₂O₆, where the *t*-ZrO₂ single phase exists up to only 5 mol% MgTa₂O₆ at 1500°C.[2] The *t*-ZrO₂ solid solutions containing up to 11 mol% YTaO₄ transform to

m-ZrO₂ with large volume expansion during cooling from 1500°C. As shown in Fig. 4, the increase in the YTaO₄ content decreases the martensitic ($t \rightarrow m$) and the reverse ($m \rightarrow t$) transformation temperatures, which are designated by M_s and A_s, respectively. The lowered transformation temperatures result in a decrease of the chemical driving force for the $t \rightarrow m$ transformation so that t-ZrO₂ phase becomes stable. Accordingly, YTaO₄ behaves as a stabilizer for t-ZrO₂.

Two phases of t-ZrO₂ and m-ZrO₂ are observed at concentrations between 12 and 14 mol% YTaO₄ after sintering for 16 h at 1500°C. A single phase of t-ZrO₂ is stabilized from 15 to 22 mol% YTaO₄ after the same sintering schedule. The t-ZrO₂ with 15 mol% YTaO₄ transforms to m-ZrO₂ during grinding. However, the t-ZrO₂ solid solutions in the composition range of 16 to 22 mol% YTaO₄ do not transform to m-ZrO₂ even for a wide range of grain sizes or aging temperatures. A typical grain size of t-ZrO₂ with 16 mol% YTaO₄ is determined to be 5 μm after sintering at 1500°C for 120 h.[11] The $t \rightarrow m$ transformation during aging at low temperatures[12,13] and the grain size dependence of the transformations[14] are characteristic of transformable t-ZrO₂. Thus, the t-ZrO₂ solid solutions stabilized in the system ZrO₂-YTaO₄ are different from the t-ZrO₂, which possesses excellent mechanical properties. From 22 mol% YTaO₄, tetragonal scheelite YTaO₄ starts to form. The room-temperature lattice parameters of the fergusonite structure YTaO₄ are determined to be $a = 5.144 \pm 0.006$ Å and $c = 10.774 \pm 0.042$ Å in this study. The two-phase field of t-ZrO₂ and tetragonal YTaO₄ extends up to about 80 mol% YTaO₄, which is not shown in Fig. 1. From this composition, a single phase of monoclinic YTaO₄ exists.

The tetragonality of t-ZrO₂ at concentrations between 14 and 22 mol% YTaO₄ increases with the YTaO₄ content, as shown in Fig. 5 and Table I. Since the fracture toughness of t-ZrO₂ alloys, stabilized at room temperature in the ZrO₂-rich region in Fig. 1, proportionally increases with their tetragonality,[3] it is expected that the toughness of t-ZrO₂ in the system ZrO₂-YTaO₄ should increase with increasing the YTaO₄ concentration in ZrO₂. As illustrated in Table I, however, the toughness decreases with increasing the tetragonality. This is because the tetragonal phase in this composition range is so stable that there is no stress-induced martensitic phase transformation, regardless of the tetragonality. Additionally, the decrease in the Young's modulus with YTaO₄ alloying causes the low calculated fracture toughness. For comparison, the fracture toughness of the transformable t-ZrO₂ alloys in the
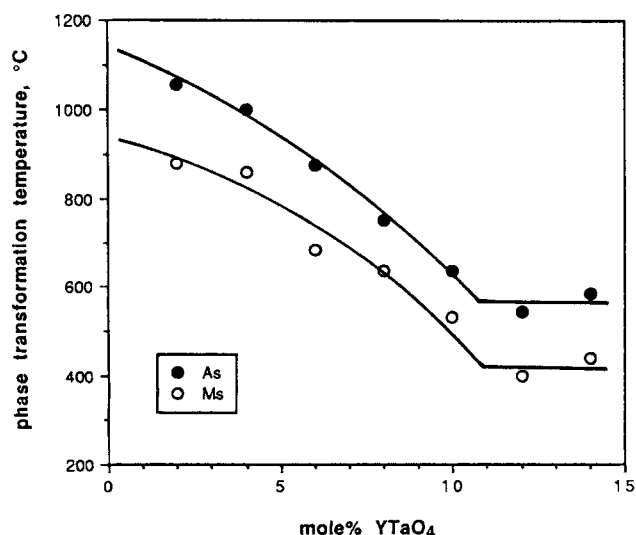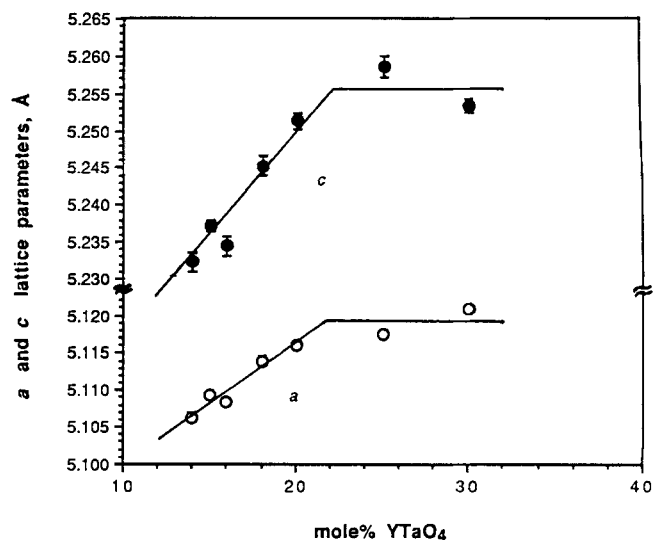

Fig. 5. a and c lattice parameters of t-ZrO₂ solid solutions in the system ZrO₂-YTaO₄.

ZrO₂-rich field of the system ZrO₂-Y₂O₃-Ta₂O₅ is determined to be 5 to 14 MPa·m$^{1/2}$ for tetragonality of 1.0141 to 1.0188, respectively, with the average Young's modulus and hardness of 210 GPa and 12 GPa.[3]

The value of 1.0203 is the largest possible room-temperature tetragonality of t-ZrO₂, which belongs to the space group $P4_2/nmc$.[3] The tetragonality of t-ZrO₂ solid solutions in the binary systems of ZrO₂ rare-earth and alkaline-earth element oxides (stabilizers) decreases toward unity, which corresponds to c-ZrO₂, as the stabilizer content increases. The lowered tetragonality by the alloying of stabilizers is consistent with an enhanced phase stability of t-ZrO₂, which is metastable at room temperature. The phase stability of t-ZrO₂ with the extraordinarily high tetragonality in the system ZrO₂-YTaO₄, which ranges from 1.0246 to 1.0264, implies that there is a difference in details of the crystal structure between two t-ZrO₂ solid solutions. Besides their lattice parameters, XRD patterns exhibit no difference in crystal structure between the transformable t-ZrO₂, alloyed with 2 mol% Y₂O₃, and the nontransformable t-ZrO₂, alloyed with 16 mol% YTaO₄, as shown in Fig. 6. The nontransformability of a similar t-ZrO₂ with an exceptionally high tetragonality of 1.0327 in the system ZrO₂-TiO₂-CeO₂ has been reported.[15] However, the nontransformability of the t-ZrO₂ in this system was related to the presence of short-range ordering of the anion lattice based on the observation of extra peaks on the XRD pattern. No such extra peaks are found from the XRD patterns of t-ZrO₂ solid solutions in the system ZrO₂-YTaO₄ in Fig. 6.

Assuming the t-ZrO₂ in the system ZrO₂-YTaO₄ was formed by a random substitution of Y³⁺ and Ta⁵⁺ for Zr⁴⁺ in eightfold coordination lattice sites, the changes in the lattice parameters (Å) as a function of mol% YTaO₄ are expected to follow the equations[3]

$$a = 5.086 + 0.00201m \qquad (2)$$

$$c = 5.189 + 0.00168m \qquad (3)$$

where m is calculated by $m = 100(\text{mol}\% \ \text{YTaO}_4)/(100 + \text{mol}\% \ \text{YTaO}_4/2)$. The slope for a axis in Eq. (2) is predicted to be larger than that for c axis in Eq. (3) but the experimental measurements in Fig. 5 exhibit a reverse trend. The poor prediction of the lattice parameters by using Eqs. (2) and (3) may be derived from a difference in either space group or mechanism for solid-solution formation between the t-ZrO₂ in the system ZrO₂-YTaO₄ and the t-ZrO₂ stabilized by rare-earth element oxides. Nevertheless, the least-squares plots of the a and c lattice constants in Fig. 5

Fig. 4. m-ZrO₂ → t-ZrO₂ (A_s) and t-ZrO₂ → m-ZrO₂ (M_s) phase transformation temperatures in the quasi-binary system ZrO₂-YTaO₄ as a function of mol% YTaO₄.

Table I. Selected Mechanical Properties and c/a Axial Ratio of t-ZrO$_2$ in the System ZrO$_2$–YTaO$_4$ Prepared by Sintering for 16 h at 1500°C

YTaO$_4$ content (mol%)	Modulus (GPa)	Hardness (GPa)	K_{Ic} (MPa · m$^{1/2}$)	c/a
14				1.0246
15	140			1.0250
16	157	11.3	5.4	1.0247
18	152	9.4	2.9	1.0257
20	144	8.8	2.5	1.0264

extrapolate to 5.083 and 5.188 Å for pure t-ZrO$_2$, respectively, which are in good agreement with the values in Eqs. (2) and (3). This indicates that the stable t-ZrO$_2$ solid solutions in the system ZrO$_2$–YTaO$_4$ are related to the crystal structure of the space group $P4_2/nmc$ so that the XRD patterns in Fig. 6 coincide. Despite the XRD patterns, the Raman spectroscopy
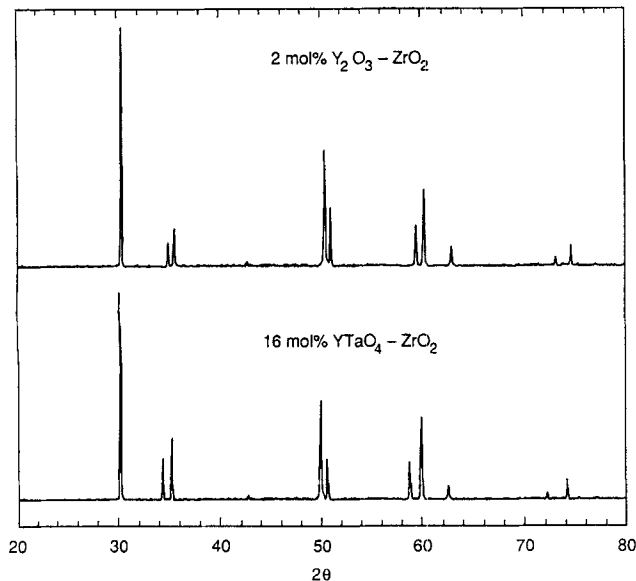
2 mol% Y$_2$O$_3$ – ZrO$_2$

16 mol% YTaO$_4$ – ZrO$_2$

20   30   40   50   60   70   80
2θ

Fig. 6. Comparison of XRD patterns of 2 mol% Y$_2$O$_3$-stabilized t-ZrO$_2$ and 16 mol% YTaO$_4$-stabilized t-ZrO$_2$.

(A) 2 mol% Y$_2$O$_3$ – ZrO$_2$

(B) 16 mol% YTaO$_4$ – ZrO$_2$

COUNT/SEC × 10^4

SCATTERING INTENSITY

200   400   600   800
WAVE NUMBER (cm^{-1})
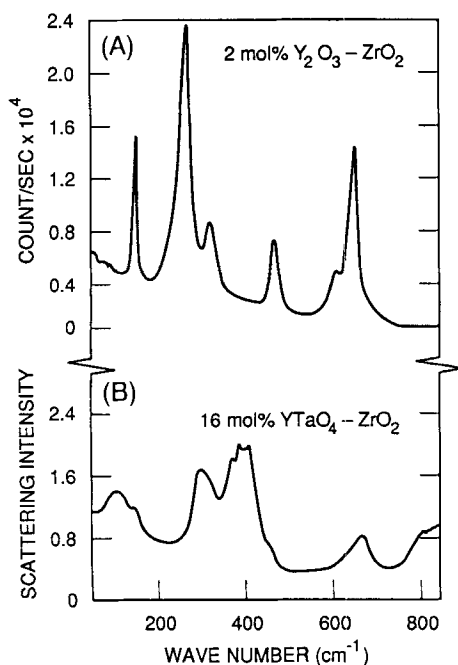
Fig. 7. Comparison of Raman spectra of (A) 2 mol% Y$_2$O$_3$-stabilized t-ZrO$_2$ and (B) 16 mol% YTaO$_4$-stabilized t-ZrO$_2$.

reveals a dissimilarity in the spectra between the transformable (with 2 mol% Y$_2$O$_3$) and the nontransformable (with 16 mol% YTaO$_4$) t-ZrO$_2$ solid solutions as shown in Fig. 7. The spectra, obtained from the 2 mol% Y$_2$O$_3$-stabilized t-ZrO$_2$, are typical of the distorted fluorite structure t-ZrO$_2$.[16] The Raman line of 466 cm^{-1} in the 2 mol% Y$_2$O$_3$-stabilized t-ZrO$_2$, which is unique for MO$_2$ oxides (M = Zr^{4+}, Ce^{4+}, Th^{4+}, U^{4+}) with the fluorite structure,[16,17] is absent in the t-ZrO$_2$ stabilized with 16 mol% YTaO$_4$. This implies that there are differences in the strength and the length of cation–oxygen ion bonds and the cation coordination between the two types of t-ZrO$_2$ solid solutions, although a close investigation should be pursued to understand the crystal structure of the t-ZrO$_2$ phase in the system ZrO$_2$–YTaO$_4$. Indeed, a small Nb^{5+} ($r_{Nb^{5+}}$ = 0.74 Å), which is similar to Ta^{5+}, most likely takes an interstitial position in the lattice of the t-ZrO$_2$, stabilized by 2 mol% Y$_2$O$_3$.[18]

In each binary system of ZrO$_2$ rare earth or alkaline earth, c-ZrO$_2$ starts to form as stabilizer content exceeds an amount for t-ZrO$_2$ single phase. In these systems, t-ZrO$_2$ is metastable at room temperature, and the tetragonality represents a degree of cubic fluorite structure distortion or microstrain due to the lattice anisotropy. Accordingly, a small tetragonality by an increased amount of stabilizer in t-ZrO$_2$ results in low phase transformability. The decreased transformability causes a small volume *fraction* of t-ZrO$_2$ to transform to m-ZrO$_2$ during the stress-induced transformation process and contributes to a low fracture toughness. In the system ZrO$_2$–YTaO$_4$, however, the tetragonal fergusonite structure YTaO$_4$ starts to form as YTaO$_4$ content exceeds the amount for t-ZrO$_2$ single phase, which is about 22 mol% YTaO$_4$ in Fig. 1. Thus, the room-temperature stable phase of t-ZrO$_2$ with the tetragonality larger than 1.0203 in the system ZrO$_2$–YTaO$_4$ is not related to a distorted form of the fluorite structure, so that the tetragonality does not represent the degree of the cubic lattice distortion. As a result, the fracture toughness of the t-ZrO$_2$ in Table I is not governed by the tetragonality.

IV. Conclusions

The phase stability of both c-ZrO$_2$ and t-ZrO$_2$ in the binary system ZrO$_2$–Y$_2$O$_3$ decreases as a result of Ta$_2$O$_5$ alloying. The t-ZrO$_2$ solid solutions in the quasi-binary system ZrO$_2$–YTaO$_4$ are characterized by their high tetragonality ($>$1.0203) at room temperature and are not related to the cubic fluorite structure. In this case the fracture toughness is low (2 to 5 MPa · m$^{1/2}$) and does not depend on the tetragonality. On the other hand, the t-ZrO$_2$ solid solutions in the system ZrO$_2$–Y$_2$O$_3$–Ta$_2$O$_5$, where Ta$_2$O$_5$ is added as a minor phase, exhibit relatively low tetragonality ($<$1.0203) at room temperature and possess a distorted cubic fluorite structure. The fracture toughness of these t-ZrO$_2$ solid solutions having tetragonality smaller than 1.0203 is high (5 to 14 MPa · m$^{1/2}$) and increases with increasing tetragonality.

References

[1]C. B. Choudhary and E. C. Subbarao, "Electrical Conduction in the Cubic Fluorite Phase in the System ZrO$_2$–YO$_{1.5}$–TaO$_{1.5}$"; pp. 665–68 in *Fast Ion Transport in Solids*. Edited by P. Vashishta, J. N. Mundy, and G. K. Shenoy.

Elsevier North Holland, New York, 1979.

[2]S. Prietzel, L. J. Gauckler, and G. Petzow, "Stability of Cubic ZrO₂ in the System ZrO₂–MgO–Ta₂O₅ and Its Electrical Conductivity"; pp. 725–29 in *Science of Ceramics*, Vol. 10. Edited by H. Hausner. Deutsche Keramische Gesellschaft, Cologne, West Germany, 1980.

[3]D.-J. Kim, "Effect of Ta₂O₅, Nb₂O₅, and HfO₂ Alloying on the Transformability of Stabilized Tetragonal ZrO₂," *J. Am. Ceram. Soc.*, **73** [1] 115–20 (1990).

[4]G. W. Jordan, M. G. McTaggart, and M. F. Berard, "Phase Distribution in the ZrO₂–Er₂O₃–Ta₂O₅ System," *J. Solid State Chem.*, **56**, 360–69 (1985).

[5]G. R. Anstis, P. Chantikul, B. R. Lawn, and D. B. Marshall, "A Critical Evaluation of Indentation for Measuring Fracture Toughness: I, Direct Crack Measurements," *J. Am. Ceram. Soc.*, **64** [9] 533–38 (1981).

[6]J. Krautkramer and H. Krautkramer, *Ultrasonic Testing of Materials.* Springer-Verlag, West Berlin, FRG, 1983.

[7]D.-J. Kim and C. R. Hubbard, "Powder X-ray Diffraction Data for Tetragonal Zirconia Solid Solutions in System ZrO₂–YTaO₄," *Powder Diffr.*, in press.

[8]D.-J. Kim, "Lattice Parameters, Ionic conductivities, and Solid Solubility Limits in Fluorite-Structure MO₂ Oxide (M = Hf⁴⁺, Zr⁴⁺, Ce⁴⁺, Th⁴⁺, U⁴⁺) Solid Solutions," *J. Am. Ceram. Soc.*, **72** [8] 1415–21 (1989).

[9]R. D. Shannon, "Revised Effective Ionic Radii and Systematic Studies of Interatomic Distances in Halides and Chalcogenides," *Acta Crystallogr., Sect. A, Found. Crystallogr.*, **32** [5] 751–67 (1976).

[10]I. A. Bondar, A. I. Kalinin, and L. N. Koroleva, "Physicochemical Investigation of the System and Synthesis of Single Crystals of a Series of Niobates," *Inorg. Mater. (Engl. Transl.)*, **8**, 1649–50 (1972).

[11]D.-J. Kim, "The Effect of Alloying on the Transformability of Y₂O₃ Stabilized Tetragonal ZrO₂"; Ph.D. Dissertation. University of Michigan, Ann Arbor, MI, 1988.

[12]T. Sato, S. Ohtaki, and M. Shimada, "Transformation of Yttria Partially Stabilized Zirconia by Low Temperature Annealing in Air," *J. Mater. Sci.*, **20**, 1466–70 (1985).

[13]T. Sato and M. Shimada, "Transformation of Ceria-Doped Tetragonal Zirconia Polycrystals by Annealing in Water," *Am. Ceram. Soc. Bull.*, **64** [10] 1382–84 (1985).

[14]A. G. Evans and R. M. Cannon, "Toughening of Brittle Solids by Martensitic Transformations," *Acta Metall.*, **34** [5] 761–800 (1986).

[15]V. C. Pandolfelli, W. M. Rainforth, and R. Stevens, "Tetragonal Zirconia Polycrystals in the ZrO₂–TiO₂–CeO₂ System"; pp. 161–65 in *Proceedings of the 1st European Ceramic Society Conference, June 18–20, 1989*, Vol. 2. Edited by G. deWith, R. A. Terpstra, and R. Metselaar. Elsevier Science Publishing, New York, 1989.

[16]D. P. C. Thackeray, "The Raman Spectrum of Zirconium Dioxide," *Spectrochim. Acta, Part A*, **30**, 549–50 (1974).

[17]V. G. Keramidas and W. B. White, "Raman Spectra of Oxides with the Fluorite Structure," *J. Chem. Phys.*, **59** [3] 1561–62 (1973).

[18]D.-J. Kim, P. F. Becher, and C. R. Hubbard, "Effect of Nb₂O₅ Alloying on Aniosotropic Thermal Expansion of 2 mol% Y₂O₃ Stabilized Tetragonal ZrO₂"; unpublished work. □